Available online at www.sciencedirect.com
SCIENCE DIRECT®
Brain Research 978 (2003) 228–232
BRAIN RESEARCH
www.elsevier.com/locate/brainres

Short communication

Rapid appearance of pathological changes of neurons and glia cells in the cerebellum of microsphere-embolized rats

Masaki Sekiguchi[a,*], Yoshiaki Sugiyama[a], Keiko Takagi[b], Norio Takagi[b], Satoshi Takeo[b], Osamu Tanaka[a], Ippei Yamato[a], Kojun Torigoe[a], R.S. Nowakowski[c]

[a]*Department of Morphology, Tokai University School of Medicine, Bohseidai, Kanagawa 259-1193, Japan*
[b]*Department of Pharmacology, Tokyo University of Pharmacy and Life Science, Tokyo, Japan*
[c]*Department of Neuroscience and Cell Biology, UMDNJ–Robert Wood Johnson Medical School, Piscataway, NJ 08854, USA*

Accepted 28 March 2003

Abstract

Neuropathological changes in the cerebellar cortex of microsphere-embolized rats were studied at 30 min and 3 h after the embolism. Necrotic processes including a sponge-like vacuolation in the molecular layer, a vague outline of some Purkinje cells, and a few pyknotic granule cells having small and dark profiles were identified at sometime between 30 min and 3 h after microsphere-induced embolism in Nissl staining. Glial fibrillary acidic protein staining shows an apparent reduction in the number of Bergmann glial processes in some of the areas where there was necrosis of the molecular layer and poor astroglia processes in the areas subjacent to the pyknotic granule cells. These data demonstrate that within a short time, microsphere-induced cerebral ischemia produces necrosis of cerebellar neurons (i.e. Purkinje and granule cells) and changes in cerebellar glia cells (i.e. Bergmann and astroglia cells), and that these neuropathological changes are secondary phenomenon caused by microsphere blockage of cerebellar blood flow.

Theme: Disorders of the nervous system

Topic: Ischemia

Keywords: Cerebral blood flow; Cerebellum; Microsphere-embolized rat

Cerebral embolism produced by the injection of microspheres into the right internal carotid artery has been shown to induce biochemical, electrophysiological, neurological and morphological abnormalities in the brain [1,4,5,11–13]. Previously, we have reported pathological characteristics induced by this model in the forebrain, including the neocortex, striatum and hippocampus [8], i.e. regions perfused by the anterior and middle cerebral arteries.

With other cerebral embolism models there are some reports of cerebellar neuropathological changes, for example, changes in Purkinje cell number after cross-clamping the ascending aorta [9,10], an increase in glial cell number after first clamping the common carotid artery and then allowing cerebral post-ischemic reperfusion [7] and a decrease of cerebellar MAP2 immunoreactivity after clamping the common carotid arteries bilaterally [6]. Therefore, the purpose of our present study is to determine whether or not microspheres injected into the internal carotid can pass though the circle of Willis and produce pathological changes in the cerebellum.

In the present study, male Wistar rats weighing 200–220 g (Charles River Japan Inc., Atsugi, Japan) were used. The animals were maintained at 23±1 °C,with a constant humidity of 55±5%, a cycle of 12 h light and 12 h darkness, and free access to food and tap water according to the *Guideline of Experimental Animal Care* issued by the Japanese Prime Minister's Office. Microsphere-induced cerebral embolism was performed by the method described previously [13]. Briefly, the rats were anesthetized with sodium pentobarbital (40 mg/kg, i.p.) and fixed in a stereotaxic holder placed on an operation plate. The right

*Corresponding author. Tel.: +81-463-93-1121, ext. 2505; fax: +81-463-92-7440.
E-mail address: smasaki@is.icc.u-tokai.ac.jp (M. Sekiguchi).

0006-8993/03/$ – see front matter
doi:10.1016/S0006-8993(03)02744-6

external carotid and pterygopalatine arteries were ligated with strings. Then a needle connected to a polyethylene catheter (3 French; Atom Co., Tokyo) was inserted into the right internal carotid artery. Nine hundred microspheres (47±0.5 μm in diameter; NEN-005, New England Nuclear Inc., Boston, MA, USA), suspended in 150 μl of a 20% dextran solution, were injected through the needle over a period of 25 s. The needle was then removed, and the wound at the injection site was closed with surgical glue. Blood flow was then restored by removing the ligatures from the arteries. It took approximately 2 min to restart the blood flow to the areas supplied by the right external carotid and pterygopalatine arteries. Two control groups were used. Sham-operated rats underwent the same operation and were injected with the same volume of vehicle but without microspheres. Additional age-matched unoperated rats were also used as controls.

A total of eight microsphere-embolized, two sham-operated and two control rats were used for histological experiments. Animals were anesthetized with Nembutal (pentobarbital sodium 50 mg/ml) and then perfused through the heart with 0.1 M sodium phosphate buffer followed by 4% paraformaldehyde in 0.1 M sodium phosphate buffer (pH 7.4). The brains were removed at either 30 min or at 3 h after the embolism. The brain was quickly dissected out and fixed for several days in 4% paraformaldehyde in 0.1 M sodium phosphate buffer (pH 7.4) at 4 °C. Then, serial 2–5-mm thick slabs were cut in the coronal plane from each brain and embedded in paraffin. Each paraffin-embedded slab was then cut serially at 7 μm. The sections were then stained with 0.5% cresyl echt violet (Nissl staining) or used for immunohistochemistry as described below.

For immunohistochemistry of glial fibrillary acidic protein (GFAP), sections were rinsed from several times in phosphate-buffered saline (PBS), treated with 0.6% Tween-20 for 30 min and then incubated in 3% normal goat serum for 30 min at room temperature. The sections were then incubated overnight with primary antibody (Sigma #G-9269; Sigma Chemical Co., Tokyo, Japan, 1:200 dilution) at room temperature. Next the sections were washed in PBS (three washes, 5 min each) and treated for 45 min with secondary antibody (biotinylated goat anti-rabbit IgG, 1:200 dilution) and then incubated for 45 min with avidin biotin peroxidase complex (ABC, 1:200 dilution) [3]. The antibody was visualized using 2–5 min incubation with the chromogen 3,3-diaminobenzidine (50 mg in 100 ml of Tris–HCl-buffered saline (TBS) and 0.01% hydrogen peroxidase). The reaction was terminated by several rinses with TBS. The sections were then counterstained with cresyl echt violet, dehydrated through a graded ethanol series, cleared in xylene, and coverslipped.

In control cerebellum, Nissl staining showed the typical three-layered organization, i.e. a single row of Purkinje cells separating the molecular layer from the granule cell layer (Fig. 1A,B and 2A). GFAP immunohistochemistry showed fine processes of Bergmann glial cells extending perpendicularly from the soma deep in the molecular layer to the pial surface (Fig. 3A), and astroglial cells within the granule cell layer extending several processes radially from the soma (Fig. 3C,D). In the cerebellum of microsphere-embolized rats, microspheres were present at the cerebellar pial surface as early as 30 min after embolism, but other pathological changes were not observed at that time (Fig. 1C,D). However, by 3 h after embolism neuropathological changes were identified in both the neuronal and glial populations in the right cerebellar hemisphere and vermis. In the molecular layer at 3 h, there was a general necrosis

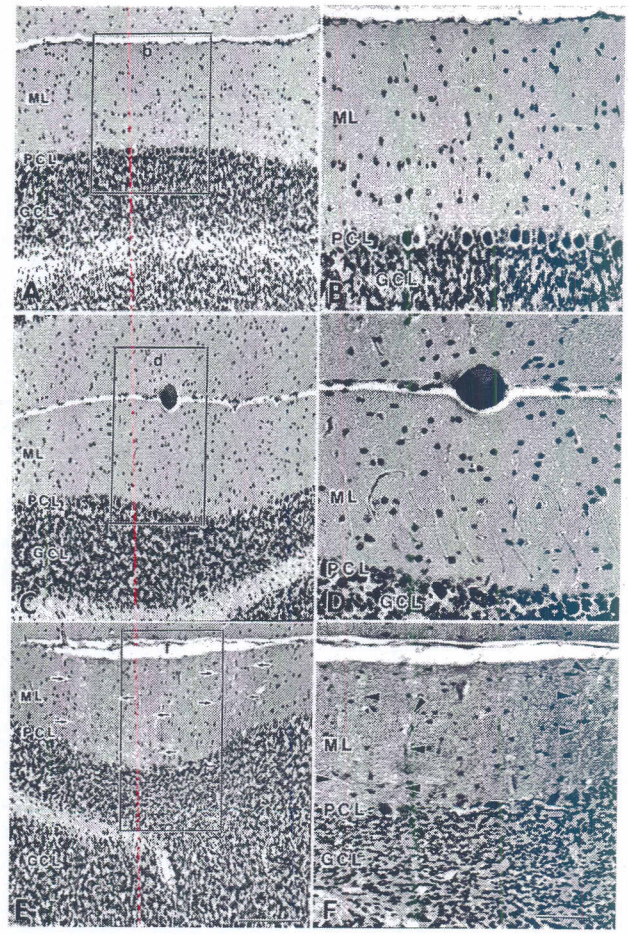

Fig. 1. A comparison of the cerebellum in control (A,B) and microsphere-embolized rats at 30 min (C,D) and at 3 h (E,F) after cerebral embolism. B is an enlargement of box 'b' in A; D is an enlargement of box 'd' in C; and F is an enlargement of box 'f' in E, respectively. A–F are all Nissl-stained sections. (A,B) Pathological changes are not observed in control cerebellum. (C,D) At 30 min after microsphere embolization, although there are microspheres at the pial surface, neuropathological changes are not observed. (E,F) At 3 h after microsphere embolization there is necrosis of the molecular layer, i.e. sponge-like vacuolation indicated by the arrows in E and the arrowheads in F. GCL, granule cell layer; PCL, Purkinje cell layer; ML, molecular layer. Scale bars: A,C,E=100 μm; B,D,F=50 μm.

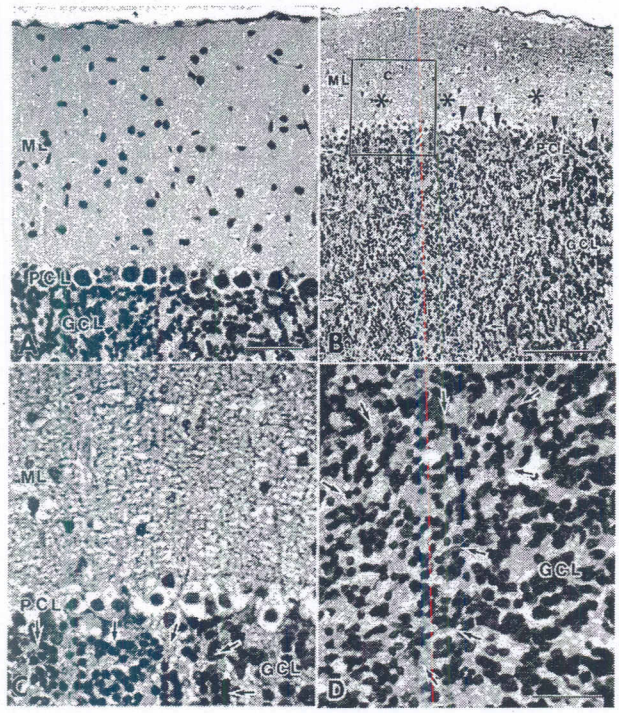

Fig. 2. A comparison of the cerebellum in control (A) and microsphere-embolized rats at 3 h (B–D) after cerebral embolism. C is an enlargement of box 'c' in B. A–D are all Nissl-stained sections. At 3 h after microsphere embolization there is a decrease in Purkinje cell number (B,C; arrowheads in B indicate the remaining Purkinje cells) and small, dark pyknotic granule cells within the granule cell layer (arrows in B–D) underlying the regions where necrosis of the molecular layer (asterisks in B) was detected. GCL, granule cell layer; PCL, Purkinje cell layer; ML, molecular layer. Scale bars: A=50 μm; B=100μm; C,D=25 μm.

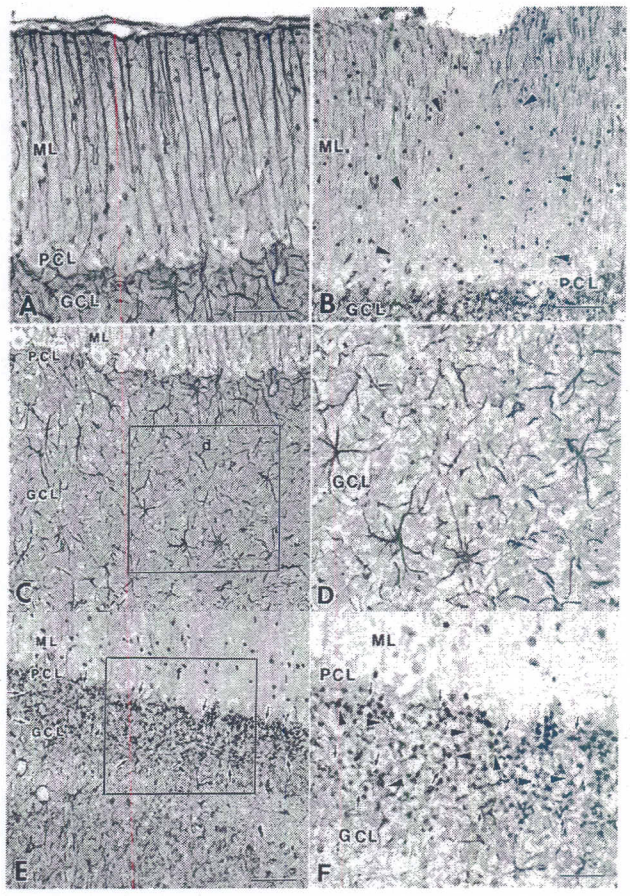

Fig. 3. A comparison of GFAP staining of the cerebellum in control (A,C,D) and microsphere-embolized rats at 3 h after cerebral embolism (B,E,F). D is an enlargement of box 'd' in C, and F is an enlargement of box 'f' in E, respectively. (A) In control cerebellum, processes of Bergmann glia cells extend perpendicularly from deeper molecular layer to the pial surface. (B) In microsphere-embolized rats, there is a partial loss of the Bergmann glial processes (GFAP-free space, arrowheads in B). (C,D) In control cerebellum, astroglia cells within the granule cells have normal processes extending in a radial direction from the somata. (E,F) In microsphere-embolized rats, there are poorly extended processes of astroglial cells (arrowheads in F; arrows in E and F indicate a group of pyknotic granule cells within the granule cell layer). GCL, granule cell layer; PCL, Purkinje cell layer; ML, molecular layer. Scale bars: A=50 μm; B=100 μm; C,E=50 μm; D,F=25 μm.

characterized by a sponge-like vacuolation (arrows in Fig. 1E, arrowheads in Fig. 1F, asterisks in Fig. 2B,C). In addition, in the areas underlying this type of necrosis there were irregularly formed Purkinje cells (Fig. 1F) or a decrease in Purkinje cell number (Fig. 2B,C). In addition, in a few cases, pyknotic granule cells could be identified as small, dark cells in the upper-middle granule cell layer (arrows in Fig. 2B–D). Importantly, both the areas of necrotic Purkinje cells and the areas containing the pyknotic granules cells were always underlying the regions where necrosis of the molecular layer was detected in Nissl staining, i.e. they were never found underlying normal areas of the molecular layer. In the glial cell population, an apparent reduction in the number of Bergmann glial processes was identified as a GFAP-free space in some of the areas where there was necrosis of the molecular layer (arrowheads in Fig. 3B). In addition, GFAP staining shows that the astrocytes in the areas subjacent to the necrotic granule cells (arrows in Fig. 3E,F) had poorly extended processes, indicating atrophy (arrowheads in Fig. 3F). The neuropathological changes of astroglia and Bergmann glia were not found in every region where pyknotic granule cells or necrosis of the molecular layer were detected; however, they were never found in association with a normal appearing molecular layer.

Interestingly, we occasionally found microspheres and microsphere-induced pathology on the left side of the cerebellum (i.e. contralateral to the injection site) and in a few areas of the midbrain (data not shown). Microspheres or microsphere-induced pathology were not found in the spinal cord or in other non-CNS organs (i.e. lung, heart, spleen, pancreas and liver).

The results show that microspheres reach the pial surface of the cerebellum and that the cerebellar cortex is clearly and rapidly affected by cerebral embolism. Since it has been previously shown that microsphere-induced le-

sions are produced mainly in ipsilateral regions of neocortex [8], striatum [8] and hippocampus [8], our results mean that microsphere injection is able to create multifocal brain infarction. In the present study, microspheres were identified at the pial surface of the cerebellum in 80% of the specimens examined at 30 min after they were injected. Neuropathological changes were present in 100% of the specimens examined at 3 h after the embolism, but were not detected at 30 min after treatment. Thus, there is a time difference between the appearance of the microspheres and the neuropathological changes, and neuropathological changes first appear sometime between 30 min and 3 h. Interestingly, microspheres and pathological changes were more frequently observed only in the right cerebellar hemisphere and/or vermis. This is consistent with the fact that we injected the right common carotid artery and with previous observations showing marked microsphere-induced neuropathology in ipsilateral regions of the brain that are supplied by the middle cerebral artery, anterior cerebral artery and posterior cerebral arteries [8].

We consider two possible routes for the microspheres to reach the cerebellum. First, it is possible, that some microspheres might enter the general circulation travel through the heart, return to the vertebral and basilar arteries and then make their way to the superior and inferior cerebellar arteries and the cerebellar cortex. If this were the case, then the microspheres would have the opportunity to reach many organs of the chest and abdomen by the general circulation. However, we could not detect the presence of microspheres or microsphere-induced pathology in any organ outside of the CNS. The alternative is that the microspheres traverse the circle of Willis (i.e. internal carotid artery→posterior communicating artery (57–61 μm)→posterior cerebral artery (114–134 μm)) into basilar artery (194–203 μm) and then enter the superior and inferior cerebellar arteries in order to reach the cerebellum. This would require that the microspheres travel against the normal direction of blood flow. This could be the case only if blood flow in these arteries is dramatically and presumably transiently affected at the time prior to and after the release of the ligation following the injection of the microspheres. Clearly, additional experiments are necessary to distinguish between these two alternatives.

The neuropathology produced by the microspheres consisted of regional changes that did not include the entire cerebellum. Importantly, despite the short survival time after the embolism, the changes were found in confined regions that generally subtended more than one cerebellar layer, always including the molecular layer and often including the underlying Purkinje and granule cells. This is consistent with the blood supply to the cerebellum. The vascular plexus of the pial branches from the superior and/or inferior cerebellar arteries consists of large vessels that run parallel to each other, supplying both the superficial and the deeper parts of the fissures, as well as smaller, interconnecting vessels [2]. From this vascular plexus branches enter the molecular layer perpendicularly. These vessels in turn branch and terminate mainly at the molecular layer, at the border between the Purkinje cell and granule cell layers, and in the cerebellar white matter [2]. Therefore, our results indicate that the microspheres block cerebellar blood flow from the pial vascular plexus; this blockage subsequently causes ischemia in a radial sector of the cerebellar cortex and produces neuropathological changes. The appearance of the neuropathological changes in the cerebellum in the period between 30 min and 3 h after microsphere-induced embolism is much sooner than the first changes reported after clamping the aorta [9,10] and the middle cerebral artery [6].

The neuropathological changes in the cerebellum included both neurons (Purkinje and granule cells) and glial cells (astroglia). However, the degeneration of astroglia or Bergmann glia cells was found in every region where necrosis of granule cells or the molecular layer was detected. Given the relatively short survival of these experiments, we suggest that the simplest interpretation of this discordance is that the neuronal pathology is induced more rapidly or more easily than the glial pathology, suggesting that neurons may be more susceptible to the ischemia that results from blocking of regional cerebellar blood flow. Alternatively, this may indicate that the glial cell degeneration is secondary to the neuronal damage. In either case, the rapidity of the onset of pathological changes and the unique geometrically regular organization of the cerebellar cortex makes it an ideal brain area for the analysis of the sequelae of microsphere-induced embolism.

Acknowledgements

Special thanks to N.L. Hayes for comment and discussion, and to S. Kobashikawa and K. Kaniwa for their technical assistance.

References

[1] A.M. Bralet, A. Beley, P. Beley, J. Bralet, Brain edema and blood brain barrier permeability following quantitative cerebral microembolism, Stroke 10 (1979) 34–38.
[2] N.G. Conradi, J. Engvall, J.R. Wolff, Angioarchitectonics of rat cerebellar cortex during pre- and postnatal development, Acta Neuropathol. 50 (1980) 131–138.
[3] S.-M. Hsu, L. Raine, H. Fanger, Use of avidin-biotin-peroxidase complex (ABC) in immunoperoxide techniques, J. Histochem. Cytochem. 29 (1980) 577–580.
[4] T. Kiyota, K. Hamajo, M. Miyamoto, A. Nagaoka, Effect of idebenone (CV-2919) on memory impairment observed in passive avoidance task in rats with cerebral embolism, Jpn. J. Pharmacol. 37 (1985) 300–302.
[5] K. Kogure, R. Busto, P. Scheinberg, Energy metabolites and water content in rat brain during the early stage of development of cerebral infarction, Brain 97 (1974) 103–114.

[6] G. Martinez, C. Giacomo, M.L. Carnazza, V. Sorrenti, R. Castana, M.L. Barcellonna, J.R. Perez-Polo, A. Vanella, MAP2, synaptophysin immunostaining in rat brain and behavioral modifications after cerebral post-ischemic reperfusion, Dev. Neurosci. 19 (1997) 457–464.

[7] G. Martinez, M.L. Carnazza, C. Di Giacomo, V. Sorrenti, M. Avitabile, A. Vanella, GFAP, S-100 and vimentin proteins in rat after cerebral post-ischemic reperfusion, Int. J. Dev. Neurosci. 16 (1998) 519–526.

[8] K. Miyake, S. Takeo, H. Kajihara, Sustained decrease in brain regional blood flow after microsphere embolism in rats, Stroke 24 (1993) 415–420.

[9] M. Sagara, M. Haraguchi, N. Yoshimura, H. Yoshida, Neuropathological changes induced by total cerebral ischemia (TCI) in a new experimental model, In Vivo 7 (1993) 493–495.

[10] M. Sato, H. Hashimoto, F. Kohsaka, Histological changes of neuronal damage in vegetative dogs induced by 18 min of complete global brain ischemia: two-phase damage of Purkinje cells and hippocampal CA1 pyramidal cells, Acta Neuropathol. 80 (1990) 527–534.

[11] T. Taguchi, N. Takagi, K. Miyake, K. Tanonaka, M. Okada, H. Kajihara, S. Takeo, Effects of naftidrofuryl oxalate on microsphere-induced changes in acetylcholine and amino acid content of rat brain regions, Exp. Brain Res. 99 (1994) 7–16.

[12] N. Takagi, K. Miyake, A. Ohiwa, R. Nukaga, S. Takeo, Effects of delayed treatment with nafronyl oxalate on microsphere embolism-induced changes in monoamine levels of rat brain regions, Br. J. Pharmacol. 118 (1996) 33–40.

[13] S. Takeo, R. Tanonaka, K. Miyake, K. Tanonaka, T. Taguchi, K. Kawakami, M. Ono, M. Hiramatsu, K. Okano, Naftidrofuryl oxalate improves impaired brain glucose metabolism after microsphere-induced cerebral embolism in rats, J. Pharmacol. Exp. Ther. 257 (1991) 404–410.

Available online at www.sciencedirect.com

SCIENCE DIRECT®

Experimental Neurology 191 (2005) 266–275

Experimental Neurology

www.elsevier.com/locate/yexnr

Time course and sequence of pathological changes in the cerebellum of microsphere-embolized rats

Masaki Sekiguchi[a,*], Keiko Takagi[b], Norio Takagi[b], Ichiro Date[b], Satoshi Takeo[b], Osamu Tanaka[a], Ippei Yamato[a], Show Kobashikawa[a], Kojun Torigoe[a], R.S. Nowakowski[c]

[a]*Department of Anatomy, Division of Basic Medicine, Tokai University School of Medicine, Bohseidai, Isehara, Kanagawa 259-1193, Japan*
[b]*Department of Pharmacology, Tokyo University of Pharmacy and Life Science, Tokyo, Japan*
[c]*Department of Neuroscience and Cell Biology, UMDNJ-Robert Wood Johnson, Medical School, Piscataway, NJ 08854, USA*

Received 27 December 2003; revised 2 September 2004; accepted 23 September 2004
Available online 10 December 2004

Abstract

Ischemia is a major cause of damage to the central nervous system as a consequence of stroke or trauma. Here, we analyzed with high temporal resolution the time course of pathological changes in the neurons (granule and Purkinje cells) and glia (Bergmann and astroglia cells) in the cerebellar cortex and white matter. The period studied ranged from 30 min to 7 days after a microsphere-induced embolism used as a model of stroke and multi-infarct dementia. Some pathological changes in the neurons in the cerebellar cortex were identified early, that is, beginning at 3 h after the microsphere-induced embolism, and glial pathology appeared only later. The pathological changes in the white matter also appeared slightly later, that is, 6 h after embolism and were less pronounced than those in the cerebellar cortex. This suggests that neuronal pathology is induced more rapidly and/or more easily than the glial pathology. In addition, BrdU staining shows that cell proliferation is limited to a 1-day period beginning about 1 day after the embolism. These data demonstrate that changes after an ischemic lesion of the cerebellum proceeds from upper cerebellar cortex to deeper cerebellar cortex or white matter and also that microsphere-induced changes proceed from neuronal to glial pathology.

Keywords: Cerebral blood flow; Neurons; Glia cells; Cerebellum; Microsphere-embolized rat

Introduction

Cerebral embolism produced by the injection of microspheres into the right internal carotid artery has been shown to induce biochemical, electrophysiological, neurological, and morphological abnormalities in the brain (Bralet et al., 1979; Kiyota et al., 1985; Kogure et al., 1974; Narumi et al., 1986; Shegel et al., 1972; Sugi et al., 1984; Taguchi et al., 1994; Takagi et al., 1996; Takeo et al., 1991, 1992). For the most part the pathological characteristics induced by cerebral embolism using microspheres have been reported in the forebrain (neocortex, striatum, and hippocampus), that is, regions perfused by the anterior or middle cerebral artery (Miyake et al., 1993). Recently, however, we showed that within a short time, microsphere-induced cerebral ischemia produced necrosis of cerebellar neurons (i.e., Purkinje and granule cells) and changes in cerebellar glia cells (i.e., Bergmann and astroglia cells) (Sekiguchi et al., 2003). Because of the unique geometrically regular architecture of the cerebellum (Palay and Chan-Palay, 1974), these observations provide insight into the mechanism related to the pathological changes following ischemia. In this manuscript, we address these changes in more detail with special emphasis on the sequence of events after the lesion. In particular, we address the important issue of whether glial cell degeneration is secondary to the neuronal damage or vice versa.

* Corresponding author. Fax: +81 463 92 7440.
E-mail address: smasaki@is.icc.u-tokai.ac.jp (M. Sekiguchi).

0014-4886/$ - see front matter © 2004 Elsevier Inc. All rights reserved.
doi:10.1016/j.expneurol.2004.09.012

Materials and methods

Animal model of microsphere-embolized rat

Male Wistar rats weighing 200–220 g (Charles River Japan Inc., Atsugi, Japan) were used; young rats were used in order to reduce the influence of aging of circulatory system. The animals were maintained at 23 ± 1°C with a constant humidity of 55 ± 5%, a light cycle of 12:12 light/dark, and ad lib food and tap water according to the "Guideline of Experimental Animal Care" issued by the Japanese Prime Minister's Office. Microsphere-induced cerebral embolism was performed as described previously (Miyake et al., 1989, 1993; Takeo, 1991; Takeo et al., 1989, 1991, 1992). Briefly, the rats were anesthetized with sodium pentobarbital (40 mg/kg, i.p.) and fixed in a stereotaxic holder placed on an operation plate. The right external carotid and pterygopalatine arteries were ligated with strings. Then a needle connected to a polyethylene catheter (3 Fr. Atom Co., Tokyo) was inserted into the right internal carotid artery. Nine hundred microspheres (47 ± 0.5 μm in diameter; NEN-005, New England Nuclear Inc., Boston, MA, USA), suspended in 150 μl of a 20% dextran solution, were injected over a period of 25 s. The needle was removed, and the wound at the injection site was closed with surgical glue. Blood flow was then restored by removing the ligatures from the arteries. With these procedures, the interruption of the blood flow within the right external carotid and pterygopalatine arteries was a total of 2 min. Sham-operated rats underwent the same operation and were injected with the same volume of vehicle without microspheres. During the entire surgical procedure body temperature, pH, PO_2, PCO_2, and other physiological parameters were monitored as described by Miyake et al. (1994); there were no differences detected between the sham-operated and microsphere-embolized rats. Additional age-matched unoperated rats were also used as controls.

Neurological and physiological assessment

At 12 h after embolism, the behavior of all operated rats was scored on the basis of (1) paucity of movement, (2) truncal curvature, and (3) forced circling during locomotion, all of which are considered to be typical symptoms of stroke in rats (Furlow and Bass, 1976; McGraw, 1997). Each symptom was ranked from 3 to 0 (3, severe; 2, moderate; 1, light; 0, faint). The sum of these scores was evaluated as a marker of neurological deficits. Rats with 7–9 symptom points were classified as type A; 4–6 points, type B; and 0–3 points, type C. To minimize variations that could result from microsphere embolism-induced pathophysiological conditions, only animals exhibiting type A neurological deficits on 12 h were selected and used for histological analysis. In previous studies (Miyake et al., 1994), neurological deficits always improved with time after the operation. Improvements in the neurological deficits with time in rats exhibiting type B and C on 1 day were faster than those of rats showing type A. No rat that demonstrated type B or C on 1 day and 3 days worsened to type A behavior on 7 days.

Histological procedures

Of a total of 67 operated animals, 7 died within 15 h of surgery and were not included in the analysis; necropsies were not performed, but indications were that the cause of death was either cerebral hemorrhage and/or respiratory failure.

Consequently, a total of 44 microsphere-embolized, 8 sham-operated, and 8 control rats, that is, three groups of rats (five or six microsphere-embolized rats, one sham-operated rat, and one control rat) at each experimental time point were used for histological observation. At 30 min, 1 h, 3 h, 6 h, 12 h, 1 day, 3 days and 7 days after the embolism, each rat was deeply anesthetized and sacrificed by intracardial perfusion with 0.1 M phosphate buffer (pH 7.4) for 30–60 s and then with 4% paraformaldehyde in 0.1 M sodium phosphate buffer (pH 7.4). The brain was removed and post-fixed for several days in 4% paraformaldehyde at 4°C. Serial 2–5 mm thick slabs were cut in the coronal plane and embedded in paraffin. Each paraffin-embedded slab was then cut serially at 7 μm. The sections were stained with 0.5% cresyl echt violet (Nissl staining) or used for immunohistochemistry as described below.

Immunohistochemical procedure

For immunohistochemistry of spot-35-calbindin (Yamakuni et al., 1984), 2′,3′-cyclic nucleotide-3-phosphodiesterase (CNPase) (Reynolds and Carey, 1989; Sprinkle et al., 1987) and glial fibrillary acidic protein (GFAP), sections from the same specimens were stained by a modification of the ABC method (Hsu et al., 1981) as follows. After several rinses in phosphate-buffered saline (PBS), sections were treated with 0.6% Tween 20 for 30 min and were incubated in 3% normal goat serum (30 min) at room temperature. The sections were then incubated overnight with one of the following primary antibodies: spot 35-calbindin for selective staining Purkinje cells and processes [Gift from T. Yamakuni (Tohoku University), 1:10,000 dilution], CNPase for selective staining of both oligodendrocytes and myelin (Sigma #G-9269, 1:250 dilution) and GFAP (Sigma #G-9269, Sigma Co., Tokyo, Japan, 1:200 dilution) at room temperature. Next, the sections were washed in PBS (three washes, 5 min each) and treated for 45 min with secondary antibody (biotinylated goat antirabbit IgG or biotinylated goat antimouse IgG, 1:200 dilution) and then incubated for 45 min with avidin biotin peroxidase complex (ABC, 1:200 dilution). The antibody was visualized using a 2- to 5-min incubation with the chromogen 3,3-diaminobenzidine (50 mg in 100 ml of Tris–HCl-buffered saline (TBS) and 0.01% hydrogen peroxidase. The reaction was stopped by

several transfers of the sections into TBS. The sections were then counterstained with cresyl echt violet, dehydrated in a graded ethanol series, cleared in xylene, and coverslipped.

Immunohistochemical procedure of TUNEL staining

For TUNEL staining, sections from the same specimens were rinsed several times in phosphate-buffered saline (PBS); sections were treated with protease K (0.02 mg/ml) for 10 min and with 3% H_2O_2 in MeOH for 5 min at room temperature and were pre-incubated with TdT buffer for 5 min. Next the sections were treated with reactive solution (DW: 39 μl, 5× buffer: 10 μl, biotinylated dUTP 1 μl, TdT enzyme 0.25 μl,) at 37°C for 2 h and the reaction was stopped with TE2N (Tris buffer: 10 mM, EDTA: 1 mM, NaCl:200 mM) for 3 min. The sections were washed in PBS (three washes, 5 min each) and incubated for 45 min with avidin–biotin–peroxidase complex (ABC, 1:200 dilution, modified from Hsu et al., 1981). The antibody was visualized using a 2–5 min incubation with the chromogen 3,3-diaminibenzidine (50 mg in 100 ml of Tris–HCl-buffered saline (TBS) and 0.01% hydrogen peroxidase. The reaction was stopped by several transfers of the sections into TBS. The sections were counterstained with Methyl green and dehydrated in a graded ethanol series, cleared in xylene, and coverslipped.

Immunohistochemical procedure of BrdU staining

To identify cells in the S-phase (DNA synthesis) of the cell cycle, 50 mg/kg of bromodeoxyuridine (BrdU, Sigma Co., B-5002) dissolved in 0.007 N sodium hydroxide was administered intraperitoneally at 30 min, 1 h, 3 h, 6 h, 12 h, 1 day, 3 days, and 7 days after the embolism. Animals were sacrificed at 30 min after the BrdU injection to localize the cells synthesizing DNA (Nowakowski et al., 1989). All animals were deeply anesthetized with ether and perfused with 4% paraformaldehyde in 0.1 M phosphate buffer. The sections were immunostained with mouse monoclonal antibody against BrdU (Becton-Dickinson, San Jose, CA) according to the procedure of Hayes and Nowakowsk (2000). A Vectastain ABC Elite Kit was used with DAB-peroxidase and nickel-cobalt intensification to demonstrate reactive sites followed by counterstaining with cresyl echt violet. To overcome masking of the BrdU antigen by formalin fixation, sections were treated with 0.1% trypsin (Sigma T-8128) in 0.1M Tris buffer, pH 7.5, containing 0.1% calcium chloride for 20 min at 37°C.

Results

Neurological assessment at 12h after surgery showed type A symptoms in approximately 81% of the specimens ($n = 36$), type B symptoms in approximately 16% ($n = 7$) and type C symptoms in approximately 4% ($n = 1$). These proportions are similar to previous results (Takeo et al., 1991). The mean neurological assessment score at 1 day was 8.0 ± 0.1. The assessment scores of rats on 3 and 7 days after the operation were decreased at 5.7 ± 0.1 and 2.6 ± 0.1, respectively. No neurological deficits were seen in any sham-operated rats.

Neurons and glial cells in control cerebellum

There were no pathological changes detected in any of the sham-operated or control rats. Routine Nissl staining showed the typical three-layered organization, and calbindin and GFAP immunohistochemistry also appeared normal (Sekiguchi et al., 2003).

General time course of pathological changes in the cerebellum after cerebellar embolism

After embolization, both the location of the type of pathology observed changed systematically with increased survival time (Table 1). At all time points, microspheres could be detected at the pia surface, within the cortex and in the surrounding fourth ventricle. Counts of microspheres were made in a standardized volume of the cerebellar cortex in each animal (Table 1). There were no statistical differences in the number of microspheres at any age (ANOVA: $F = 0.545$, $P > 0.788$) indicating that they remained without resolving into the blood vessels. Most of the microspheres and the associated pathological changes were observed in the ipsilateral cerebellar hemisphere and vermis of the cerebellum, however, in two specimens (one at 6 h and another at 12 h) microspheres and pathology were observed both contralaterally and ipsilaterally (Fig. 1).

A summary of the onset and general time course of the pathological changes detected is shown in Table 1. This summary shows that each type of pathological change has a specific time of onset. Typically, after the onset there was a gradual increase in the severity of the pathological change over the next few sampled time points (Fig. 1). The types of pathological changes and the timing of their onset are described fully below.

Time course of pathological changes in the cerebellum after embolism

Thirty minutes and 1 hour after embolization

The only detectable pathology at 30 min or 1 h after embolization was the presence of sponge-liked coarsened fibers (malacia) of the molecular layer seen in Nissl stains in one specimen at each time point.

Three hours after embolization

At 3 h after embolism, in routine Nissl staining, focal necrosis of the molecular layer, pyknotic appearance of a few granule cells within the superficial and/or middle part

Table 1
Presence of microspheres, and onset and degree of pathological changes at 8 time points

	30 min	1 h	3 h	6 h	12 h	1 day	3 days	7 days	Sham operation or control rats
Number of animals showing presence of microspheres and/or pathological changes	4/5 (only microsphere)	4/5 (only microsphere)	3/5 (60%)	4/5 (80%)	3/6 (50%)	5/6 (83%)	3/6 (50%)	3/6 (50%)	0%
Number of microspheres (standard volume 300 μm thick)	26	6	20.3	19.3	24.3	28	14	17.3	0
Changes in the molecular layer	+	+	+	++	++	+++	+++	+++	–
Necrosis or loss of Purkinje cells (calbindin staining)	–	–	+	+	++	++	++	++	–
Loss of Purkinje cell dendrites (calbindin staining)	–	–	+	+	++	+++	+++	+++	–
Necrosis or TUNEL-positive granule cells (Nissl · TUNEL staining)	–	–	+	+	++	+++	+++	+++	–
Loss of Bergmann glia processes (GFAP staining)	–	–	+	+	+	++	++	++	–
Loss of astroglia cells within the granule cell layer (GFAP staining)	–	–	+	+	+	++	++	++	–
Loss of Bergmann glia soma (S-100 staining)	–	–	–	–	+	++	++	++	–
Loss of astroglia soma or TUNEL-positive astroglia cells within the granule cell layer (GFAP · TUNEL staining)	–	–	–	–	+	++	++	++	–
Vacuoles or demyelination of white matter (Nissl · CNPase staining)	–	–	–	+(subtle)	+	++	++	++	–
Cell proliferation	–	–	–	–	–	+	–	–	–

–: none, +: weak, ++: moderate, +++: intense.

of the granule cell layer could be detected. Also, in areas adjacent to the focal necrosis of the molecular layer spaces there were "missing" Purkinje cell somata in some but not all specimens. Staining with calbindin showed fragmentation of Purkinje cell dendrites in these areas (arrowheads in Fig. 2A), and, importantly, Purkinje cells not located near an area of focal necrosis showed no changes. With TUNEL-staining, a small number of TUNEL-positive cells (arrows in Fig. 2C) was also detected in upper part of the granule cell layer, that is, in the same areas where pyknotic granule cells were seen. Staining with GFAP showed breaks in the normal palisades forming GFAP-free spaces in the areas of focal necrosis, indicating the loss of Bergmann glial processes (arrowheads in Fig. 2E). Finally, astrocytes in the areas subjacent to the necrotic granule cells (area indicated by the arrowheads in Fig. 2G) were atrophied with poorly extended processes (arrows in Fig. 2G).

Six hours after embolization

All of the pathology seen at 3 h is also present at 6 h. In addition, we also detected subtle necrosis with small vacuoles of the white matter at this time point and slight demyelination assessed by CNPase appeared. The other pathological features were generally more severe than seen at 3 h. For example, TUNEL-positive cells were now detected in the molecular layer in addition to the upper portion of the granule cell layer. Disruption of the Purkinje cell layer was detected by disappearing soma. Also, the atrophy of astrocytes in the areas subjacent to the necrotic granule cells was more severe with thinner and more fragmentation of the processes than was seen at 3 h.

Finally, in double immunohistochemistry for GFAP and TUNEL staining, TUNEL-positive/GFAP-negative (arrowheads of Figs. 4G and H, data of 6 h is not shown). In contrast, most astroglia cells (arrows of Figs. 4G and H, data of 6 h is not shown) could be found as GFAP-positive/TUNEL-negative in the regions where the focal necrosis of the granule cells was detected (indicated by the arrowheads in Fig. 4F, data of 6 h is not shown). A few GFAP-positive/TUNEL-positive astroglia cells were also present, and consistent with their glial identity, were clearly smaller than the TUNEL-positive/GFAP-negative granule cells (Figs. 4G and H, data of 6 h are not shown).

Twelve hours after embolization

At 12 h after embolization the focal necrosis of the molecular layer and loss and atrophy of Purkinje somata and loss of dendritic process of Purkinje cells was more intense than at 6 h. There were also both qualitative and intensity changes in some of the other pathology. For example, the pyknotic and TUNEL-positive granule cells now appeared in the deeper portion of granule cell layer (GCL), and the necrosis and vacuolation of the white matter of the cerebellum became more intense. CNP-ase staining which was faint at 6 h is now quite strong confirming the presence of demyelination of the white

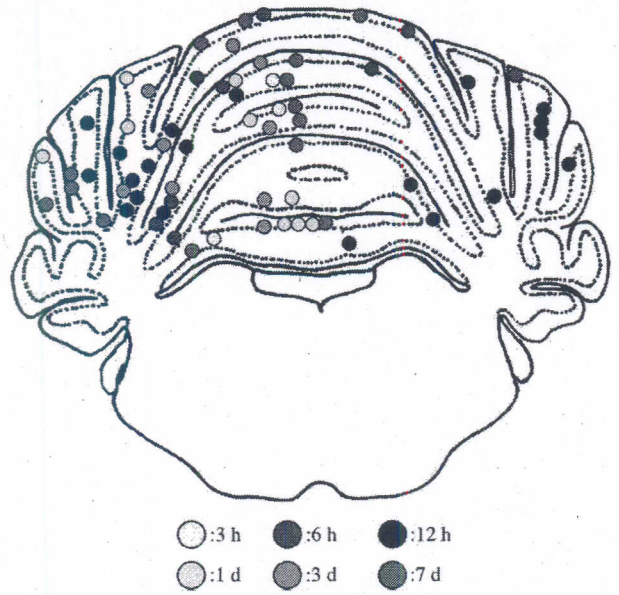

Fig. 1. Summary of the location of cerebellar changes as a function of time. The sky blue circles indicate the changes at 3 h.; the blue circles at 6 h; the dark blue circle at 12 h; the yellow circle at 1 day; the orange circle at 3 days; and the pink circles at 7 days. This summary is derived from a total of five samples at each time stages. Most of the pathology was found in the right cerebellar hemisphere and/or vermis, that is, ipsilateral to the perfusion blockage, except for a few locations at 6 and 12 h after the embolism.

matter. Also, the loss of Bergmann glial processes as seen with GFAP staining as well as the vacuolation of the molecular layer were larger and more widespread than at 3 or 6 h. Again, the degeneration of astroglia has progressed as the astroglia cell processes are now even thinner and show more fragmentation than at 3 h.

One day after embolization

At 1 day after embolization, all the pathological changes seen at 12 h are present and for the most part they are more intense than at 3 or 12 h (compare Fig. 2C with D; compare Fig. 2E with F, Figs. 3A, B). In addition, there is one notable new pathological indicator, namely, a few BrdU-positive cells were detected in the outer part of the molecular layer of the regions where the focal necrosis of the molecular layer was detected and near the pial surface at 1 day after embolization (area enclosed by box in Figs. 4A, B and arrowheads in 4C). No BrdU-positive cells were found at any other survival times.

Three and seven days after embolization

At 3 and 7 days after embolization, all of the pathological features detected earlier in the time course with the exception of the presence of cell proliferation persisted (Figs. 2B, H). A few interesting qualitative changes were found. For example, in some samples at 3 days after embolization, focal necrotic areas are surrounded by clusters of cells (asterisk and arrows in Figs. 3C and D). The cells in these clusters did not stain with anti-GFAP (not illustrated) or anti-CNPase (asterisk and arrows in Fig. 3D). Generally, necrosis and vacuolation of the white matter of the cerebellum was found in the ipsilateral hemisphere.

Discussion

It has been shown that the embolism model of small microclots has value for formation of random infarcts throughout the brain (Lapchak and Araujo, 2001; Zivin et al., 1985) or testing the effects of drug combinations or neuroprotective agents plus a thrombolytic. In contrast, non-dissolving microspheres such as those used in present study remain within the blood vessels of the brain or in the cerebral ventricles. This produces sustained cerebral ischemia and induces the widespread formation of small emboli and multiple infarct areas in the brain (Miyake et al., 1993). Thus, this model is considered to mimic focal ischemia-induced human stroke (Lyden et al., 1992) or multi-infarct dementia (Naritomi, 1991). Such irreversible cerebral embolism shows clear damage in the brain and leads to learning and memory dysfunction (Nagakura et al., 2002; Takagi et al., 1997).

We used a time course analysis with closely spaced intervals to study the sequence of events that occur in the cerebellum between 30 min and 7 days after embolism with microspheres. During this interval, the number of microspheres within cerebellar vasculature was unchanged at all experimented stages. This confirms that the microspheres produce a stable long lasting injury to the cerebellum, and corroborates a previous study of Morii (1992) with carbon microspheres. Importantly, in the animals used in the present study, there was infarction of widespread areas including cerebral cortex, hippocampus, corpus striatum, midbrain, cerebellum, and medulla from the injection of only 900 microspheres (data not shown).

Within the cerebellum, we were able to show that there was: (1) a decrease in the number of Bergmann glia cells in regions where there was focal necrosis of the molecular layer, (2) a decrease in the number of astrocytes in the regions where the focal necrosis of the granule cell layer was detected, (3) a transient period of cell proliferation, and in general, no evidence for compensatory phenomena such as increased production of glia cells or blood vessel, (4) appearance of demyelination in the white matter, (5) a disappearance of some Purkinje cell soma and dendritic process and an increase TUNEL-positive cells in the granule cell layer, and (6) the appearance of some neuronal pathology in the molecular layer, and for both the granule and Purkinje cells in *contralateral* cerebral cortex. Each of these pathologies appeared at a characteristic time after the embolism (see Table 1) and we interpret the onset of each event as a useful indicator of the sequence of events occurring after embolization.

The pathological changes in the cerebellum involved both neurons (Purkinje and granule cells) and glial cells

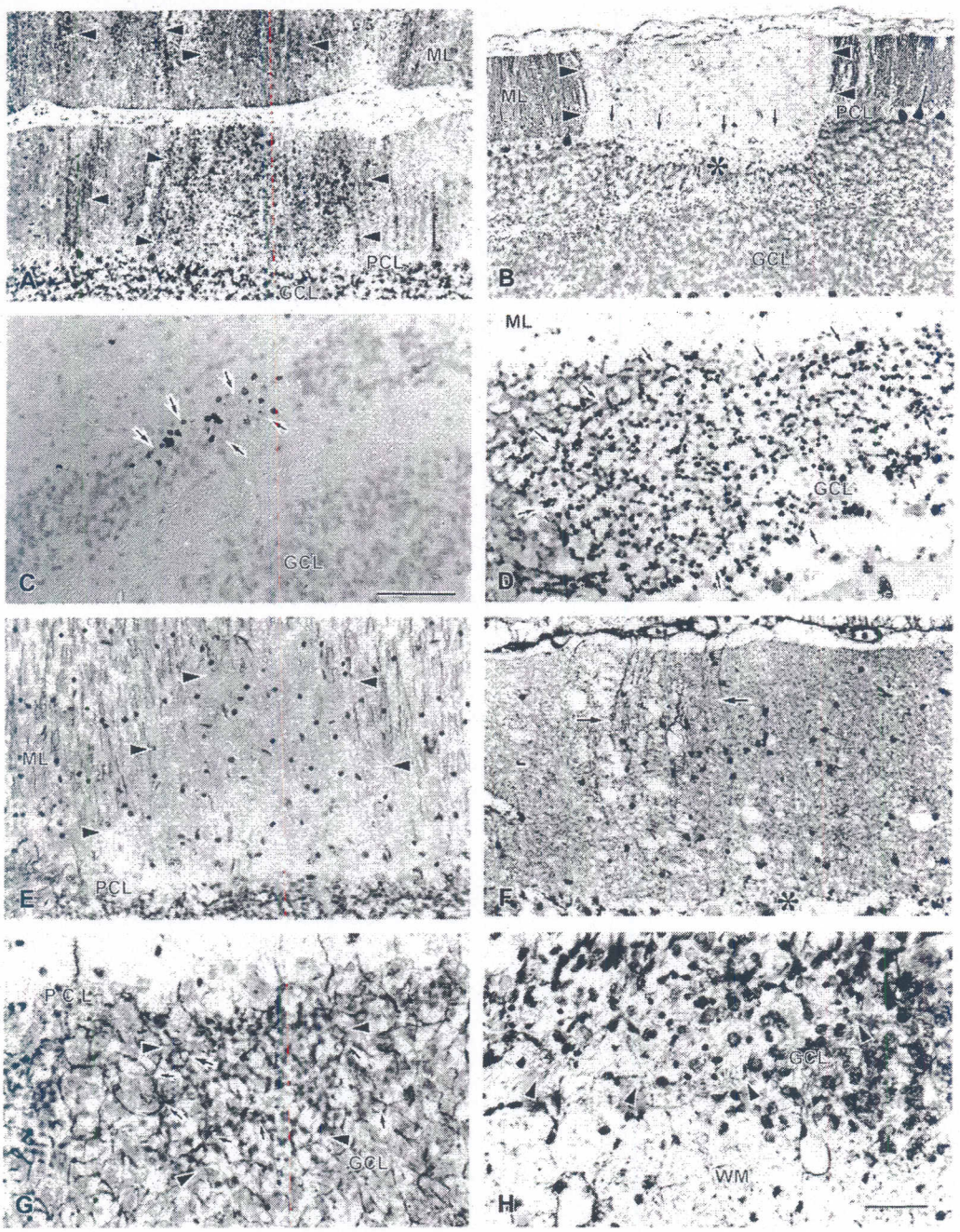

Fig. 2. The time course of pathological changes in the Purkinje cells (A, B) and in the granule cell layer (C, D), in the Bergmann glia cells (E, F) and in the astroglia cells of the granule cell layer (G, H) after cerebral embolism as seen with anti-calbindin, anti-TUNEL and anti-GFAP respectively. A, C, E, and G are at 3 h, D and F are at 1 day and B and H are at 7 days after embolism. A: dendritic fragmentation of Purkinje cells (deeply staining area indicated by arrowheads) can be seen. B: the loss of both dendrite (arrowheads) and Purkinje cell soma (arrows) can be seen. C: TUNEL-positive granule cells (arrows in C) are found in upper part of the granule cell layer. D: many TUNEL-positive granule cells (arrows in D) are found throughout the granule cell layer. E: there is a partial loss of Bergmann glia processes (arrowheads show a GFAP-free space). F: loss of Bergmann glia processes (arrows in F indicate remained Bergmann glia processes). Also, the necrosis with vacuoles of the molecular layer are more widespread than at 3 h. G: poorly extended processes of astroglia cells processes (arrows) seen in the areas subjacent to the necrotic granule cells (arrowheads). H: soma and processes of astroglia cells are decreased extremely in the areas subjacent to the necrotic granule cells (arrowheads of H). Abbreviations: GCL: granule cell layer, ML: molecular layer, PCL: Purkinje cell layer, WM: white matter. Scale bars: A–D = 100 μm, E, F = 50 μm, G, H = 25 μm.

(Bergmann and astroglia cells). From the onset of the pathology (Table 1), it seems clear that the neuronal pathology precedes the glia pathology. We found the first pathological changes in the molecular layer within 30 min and pathology in the Purkinje cell layer and the appearance of pyknotic granule cells first occur sometime between 1

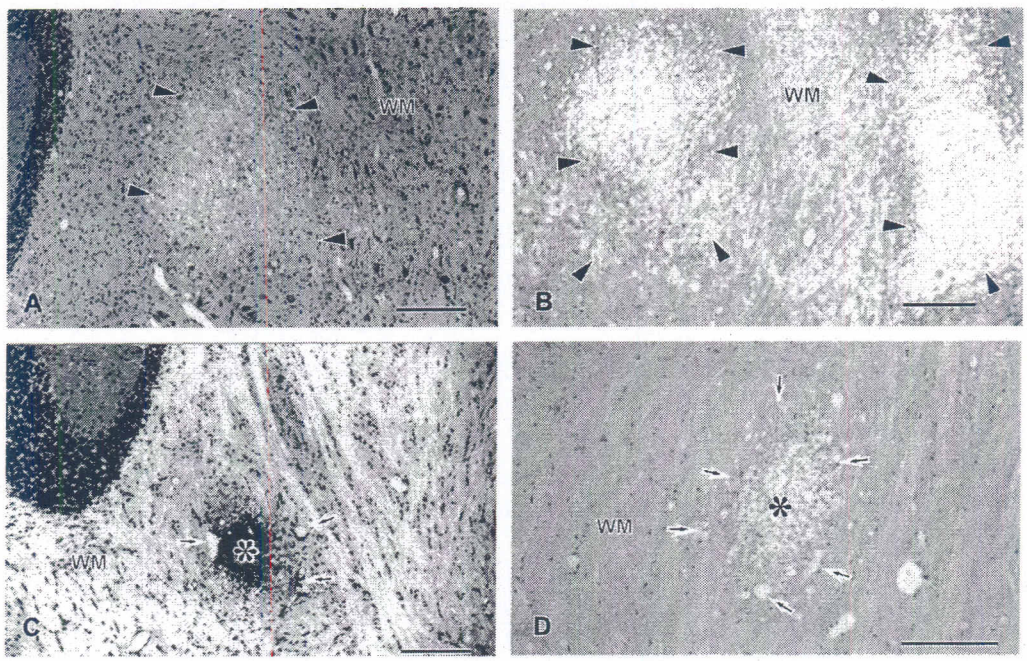

Fig. 3. Pathological changes in the cerebellar white matter after cerebral embolism (A–D). A and B are sections at 1 day and C and D are sections at 3 days after embolism. A and C are Nissl-stained; B and D are adjacent to A and C, respectively, and are stained by CNP-ase immunohistochemistry. A and B: intense necrosis with large vacuoles of white matter (arrowheads in A) is found adjacent to the deep cerebellar nuclei and demyelination (arrowheads in B) is associated with these necrotic vacuoles. C and D: necrosis with very small vacuoles (arrows in C and D) and a surrounding cell cluster are found in the white matter (asterisk in C and D); this cluster of cells does not stain with anti-CNP-ase immunohistochemistry and does not have obvious demyelination (D). Abbreviations: WM: white matter. Scale bars: A, B, C = 200 μm, D = 100 μm.

and 3 h, which confirms our previous study (Sekiguchi et al., 2003). In addition, for both neurons and glia, pathology in the processes appears prior to pathology in the somata (Table 1) indicating an intracellular progression of the reaction to injury. For example, glial cell reactions (i.e., disappearance of glia processes) first becomes evident between 1 and 3 h after embolism, however, the disappearance of glia somata does not becomes evident until 12 h–1 day after embolism. The simplest interpretation of this sequence of events is that the neuronal pathology is induced more rapidly or more easily than the glial pathology. This would indicate that neurons may be more susceptible to the ischemia that results from blocking regional cerebellar blood flow. In addition, this may indicate that the glial cell degeneration is secondary to the neuronal damage. This latter idea is supported by the recent immunohistochemical analysis using two neuronal markers (NeuN and microtubule-associated protein 2 (MAP-2) and GFAP of astroglia cell maker (Lee et al., 2003). In this analysis of early reperfusion following severe focal cerebral ischemia (middle cerebral artery), two neuronal markers were both greatly reduced by 1 h after reperfusion and declined further at 3 h. In contrast, immunoreactivity for the astrocytic marker, GFAP, was preserved in all tissue that had been subjected to severe ischemia and labeling of another astrocytic protein, glutamine synthetase, was not increased until 3 h after reperfusion (Lee et al., 2003).

The onset of pathology in the cerebellar white matter first became evident at 6 h after the microsphere injection (Table 1). These changes involved demyelination of nerve fibers and was not accompanied by any detectable changes in the glia cells. This may indicate either (1) that regions of deeper cerebellar white matter may be less sensitive to the blocking of blood flow than the superficial cerebellar regions are; perhaps, because the vascular plexus of both inferior and superior arteries enter the molecular layer and branch or terminate at the border between Purkinje and granule cells and in the superficial cerebellar white matter (Conradi et al., 1980), or (2) the changes of the white matter are induced indirectly by loss of Purkinje cell axon from the degeneration of the Purkinje cell somata. We consider the second possibility to be more likely, but additional observations are necessary to confirm this.

Finally, cell proliferation as detected by the presence of BrdU positive cells was detected in the outer part of the molecular layer of the cerebellum and pial surface at only a single time point beginning at 1 day after embolization. No BrdU-positive cells were found at 3 days or at any other survival time. Thus, BrdU staining shows that cell proliferation occurs only transiently after the injury. In addition, because it is relatively late in the process (see Table 1), it must be fairly far down in the cascade of events occurring after embolism. Interestingly, in the neocortex, striatum, and hippocampal formation of the same specimens, there were many of BrdU positive cells at

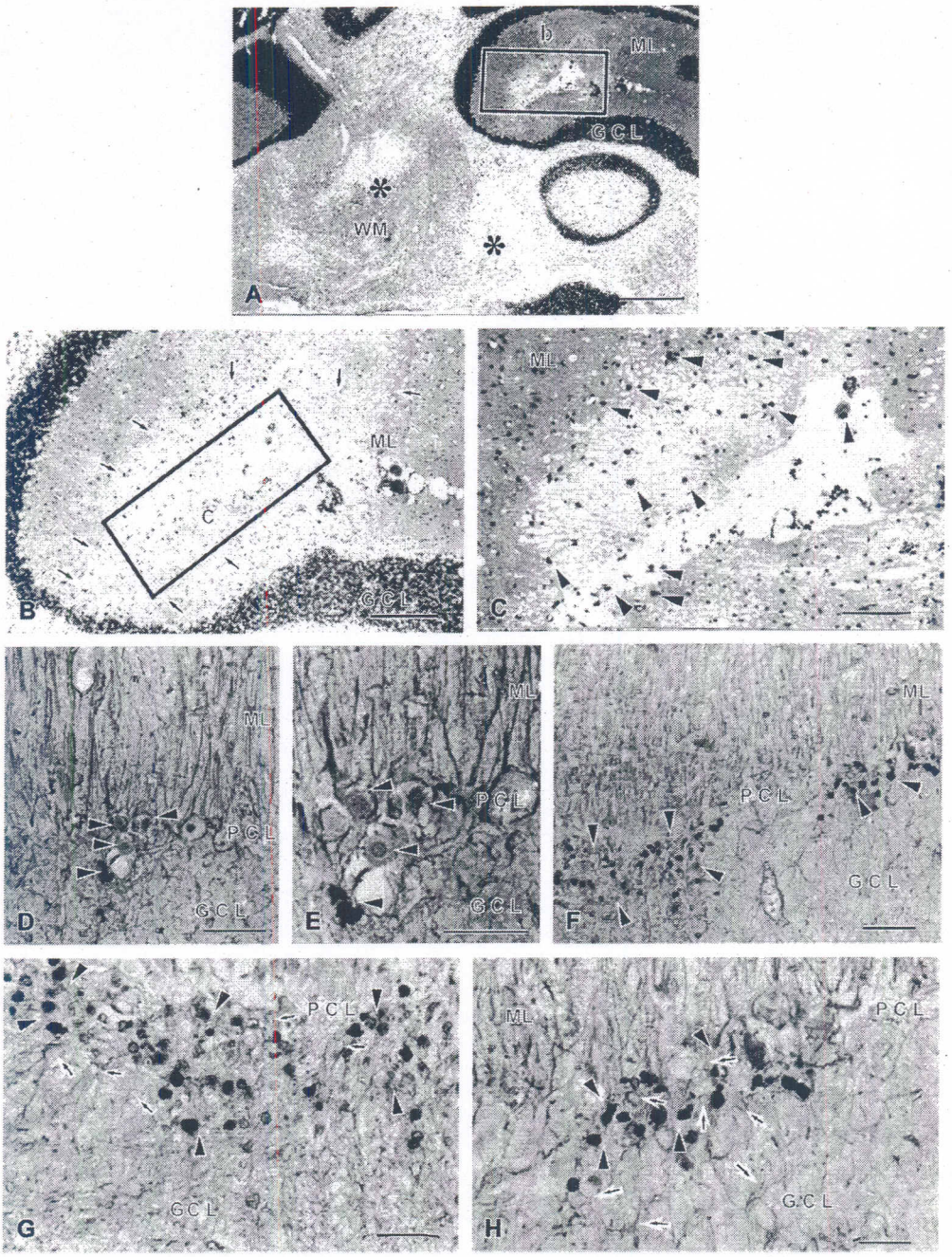

Fig. 4. BrdU-positive cells in the molecular layer of the cerebellum (A–C) and double staining of GFAP and TUNEL staining (D–H). A–C are sections of 1 day after cerebral embolism and D–H are sections of 12 h after cerebral embolism. B is an enlargement of box b in A and C is an enlargement of box c in B, respectively. A: there is necrosis of the molecular layer (box b) and of white matter (asterisk in A) of the cerebellum. B and C: arrows in B indicate an area of necrosis of the molecular layer and a few BrdU-positive cells (arrowheads in C) are found in the upper part of the molecular layer and near the pial surface. D and E: a few granule cells are TUNEL-positive (arrowheads in D and E). Note that adjacent Bergmann and astroglia soma that are TUNEL-negative extend their processes normally. Also, there are a few necrotic-like Purkinje cells (arrowheads in D and E). F–H: some of granule cells are TUNEL-positive (arrowheads in F, G, and H), although adjacent Bergmann and most of astroglia cells (arrows in H) are TUNEL-negative; TUNEL-negative astroglia soma, and GFAP-positive astroglia processes can also be seen. GCL: granule cell layer, ML: molecular layer, PCL: Purkinje cell layer, WM: white matter. Scale bars: A = 500 μm, B = 100 μm, C, E = 50 μm, D, G, H, F = 25 μm.

several times after embolism (Sekiguchi et al., unpublished observations).

Taken together, these data indicate that the cerebellum exhibits a sequence of tissue damage with neuronal damage appearing first and glial cell damage appearing later. Interestingly, within the different populations of neurons there also was differential susceptibility. Specifically, pyknotic granule cells were evident from 3 h after embolism

by TUNEL staining, but dying Purkinje cells were not present until about 12 h and the number of weak dying Purkinje cells was small even in this point (see Figs. 4D and E). The changes in the Purkinje cells followed a drawn out time course. Interestingly, the first changes were evident in the Purkinje cell's processes early, that is, between 1 and 3 h, and only later, that is, beginning 6–12 h after embolism and extending through at least 7 days, did the disappearance of Purkinje soma became evident. At no time was evidence of TUNEL staining seen in the Purkinje cell population. This sequence is similar to that reported by Martin et al. (2000). In addition, Martin et al. (2000) also reported that degenerating Purkinje cells were necrotic and degenerating granule cells were apoptotic (Martin et al., 2000). It is likely that this difference in the mode of cell death explains why we did not find TUNEL-positive Purkinje cells at any time during our analysis.

Most pathological changes were found in the ipsilateral cerebellum and/or medulla (data from medulla are not shown). However, at 6 and 12 h after the injection of the microspheres, 5 of 44 specimens showed damage in the contralateral cerebellum and/or medulla (data from medulla are not shown). This is an incidence of 11%, which is similar to a previous report of about a 10% incidence of microsphere-induced damage in the contralateral cerebral cortex following an intracarotid injection (Morii, 1992). It is not known why damage induced by microspheres was observed in the contralateral cerebellum. Previously, we considered two possible routes for the microspheres to reach the cerebellum (Sekiguchi et al., 2003). First, it is possible that some microspheres might enter the general circulation travel through the heart, return to the vertebral and basilar arteries, and then make their way to superior and inferior cerebral arteries and the cerebral cortex. If this were the case, then microspheres would have the opportunity to reach both sides of the cerebellum and would also reach many organs of the chest and abdomen by the general circulation. However, we could not detect the presence of microspheres and microsphere-induced pathology in any organ outside of brain (Sekiguchi et al., 2003). The alternative route is that in some specimens during a short interval after the release of the ligation following the injection of the microspheres, the blood pressure is changed transiently, resulting in a reversal of blood flow (Sekiguchi et al., 2003); this would allow microspheres to reach the cerebellum and would also account for the ipsilateral and contralateral infarcts. We have not yet studied the pressure, speed, or direction of blood flow following our lesion. Also, the number of specimens that we have exhibiting contralateral damage is still too few to evaluate in order to have a detailed time course of pathological changes contralaterally; thus, additional insight into this interesting issue cannot be provided from this study.

In summary, we have demonstrated a characteristic sequence of appearance of pathological events in the cerebellar cortex following a microsphere-induced embolism. First, neuronal pathology has an early onset, that is, appearing within 30 min to 3 h after embolism. Second, glial cell damage (loss of soma and processes) appears only later, that is, between 3 h and 1 day after embolism. Third, there is no clear proliferative glial cell response (e.g., as part of a repair process) except for a short and transient appearance of a small number of proliferating cells at 1 day after injury. The fact that pathological changes in cerebellar neurons are induced more rapidly than the glial cells indicates that neurons may be more susceptible to the ischemia that results from blocking regional cerebellar blood flow.

References

Bralet, A.M., Beley, A., Beley, P., Bralet, J., 1979. Brain edema and blood brain barrier permeability following quantitative cerebral microembolism. Stroke 10, 34–38.

Conradi, N.G., Engvall, J., Wolff, J.R., 1980. Angioarchitectonics of rat cerebellar cortex during pre- and postnatal development. Acta Neuropathol. 50, 131–138.

Furlow, T.W., Bass, N.H., 1976. Arachidonate-induced cerebrovascular occlusion in the rat. Neurophysiology 26, 297–304.

Hayes, N.L., Nowakowsk, R.S., 2000. Exploiting the dynamics of S-phase tracers in developing brain: interkinetic nuclear migration for cells entering versus leaving the S-phase. Dev. Neurosci. 22, 44–55.

Hsu, S.-M., Raine, L., Fanger, H., 1981. Use of avidin–biotin–peroxidase complex (ABC) in immunoperoxidase techniques. J. Histochem. Cytochem. 29, 577–580.

Kiyota, T., Hamajo, K., Miyamoto, M., Nagaoka, A., 1985. Effect of idebenone (CV-2919) on memory impairment observed in passive avoidance task in rats with cerebral embolism. Jpn. J. Pharmacol. 37, 300–302.

Kogure, K., Busto, R., Scheinberg, P., 1974. Energy metabolites and water content in brain during the early stage of development of cerebral infarction. Brain 97, 103–114.

Lapchak, P.A., Araujo, D.M., 2001. Reducing bleeding complications after thrombolytic therapy for stroke: clinical potential of metalloproteinase inhibitors and spin trap agents. CNS Drugs 15, 819–829.

Lyden, P.D., Zivin, J.A., Chabolla, D.R., Jacobs, M.A., Gage, F.H., 1992. Quantitative effects of cerebral infarction on spatial learning in rats. Exp. Neurol. 116, 122–132.

Lee, D.R., Helps, S.C., Gibbins, I.L., Nilsson, M., Sims, N.R., 2003. Losses of NG2 and NeuN immunoreactivity but not astrocytic markers during early reperfusion following severe focal cerebral ischemia. Brain Res. 989, 221–230.

Martin, L.J., Sieber, F.E., Trystman, R.J., 2000. Apoptosis and necrosis occur in separate neuronal populations in hippocampus and cerebellum after ischemia and are associated with differential alterations in metabotropic glutamate receptor signaling pathways. J. Cereb. Blood Metab. 20, 153–167.

McGraw, C.P., 1997. Experimental cerebral infarction: effect of pentobarbital in Mongolian gerbils. Arch. Neurol. 34, 334–336.

Miyake, K., Tanonaka, K., Minematsu, R., Inoue, K., Takeo, S., 1989. Possible therapeutic effect of naftidrofuryl oxalate on brain energy metabolism after microsphere-induced cerebral embolism. Br. J. Pharmacol. 98, 389–396.

Miyake, K., Takeo, S., Kajihara, H., 1993. Sustained decrease in brain regional blood flow after microsphere embolism in rats. Stroke 24, 415–420.

Miyake, K., Takagi, N., Takeo, S., 1994. Effects of naftidrofuryl oxalate on microsphere embolism-induced decrease in regional blood flow of rat brain. Br. J. Pharmacol. 112, 226–230.

Morii, K., 1992. Pathological and pathophysiological studies on central

nervous system in experimental cerebral ischemia of the rat. Hokkaido J. Med. 67, 109–129.

Nagakura, A., Takagi, N., Takeo, S., 2002. Impairment of cerebral cAMP-mediated signal transduction system and of spatial memory function after microsphere embolism in rats. Neuroscience 113, 279–287.

Naritomi, H., 1991. Experimental basis of multi-infarct dementia: memory impairments in rodent models of ischemia. Alzheimer Dis. Assoc. Disord. 5, 103–111.

Narumi, S., Kiyota, Y., Nagaoka, A., 1986. Cerebral embolization impairs memory function and reduces cholinergic marker enzyme activities in various brain regions in rats. Pharmacol. Biochem. Behav. 24, 1729–1731.

Nowakowski, R.S., Lewin, S.B., Miller, M.W., 1989. Bromodeoxyuridine immunohistochemical determination of the lengths of the cell cycle and the DNA-synthetic phase for an anatomically defined population. J. Neurocytol. 18, 311–318.

Palay, S.L., Chan-Palay, V., 1974. Cerebellar Cortex, Cytology and Organization. Springer-Verlag, New York.

Reynolds, R., Carey, E.M., 1989. Herschkowitz N: immunohistochemical localization of myelin basic protein and 2′, 3′-cyclic nucleotide 3′-phosphohydrolase in flattened membrane expansions produced by cultured oligodendrocytes. Neuroscience 28, 181–188.

Sekiguchi, M., Sugiyama, Y., Takagi, K., Takagi, N., Takeo, S., Tanaka, O., Yamato, I., Torigoe, K., Nowakowski, R.S., 2003. Rapid appearance of pathological changes of neurons and glia cells in the cerebellum of microsphere-embolized rats. Brain Res. 978, 228–232.

Shegel, B.A., Meidinger, R., Elliott, A.J., Studer, R., Curtis, C., Morgan, J., Potchen, J., 1972. Experimental cerebral microembolism: multiple tracer assessment of brain edema. Arch. Neurol. 26, 73–77.

Sprinkle, T.J., Agee, J.F., Tippins, R.B., Chamberlain, C.R., Faguet, G.B., De Vries, G.H., 1987. Monoclonal antibody production to human and bovine 2′:3′-cyclic nucleotide 3′-phosphosiesterase (CNPase): high-specificity recognition in whole brain acetone powders and conservation of sequence between CNP1 and CNP2. Brain Res. 426, 349–357.

Sugi, T., Schuier, F.J., Hossmann, K.A., Zulch, K.J., 1984. The effect of mild microembolic injury on the energy metabolism of the cat brain. J. Neurol. 223, 285–292.

Taguchi, T., Miyake, K., Tanonaka, K., Okada, M., Horiguchi, T., Takagi, N., Fujimori, K., Miyake, K., Takeo, S., Kajihara, H., 1994. Sustained decrease in brain regional blood flow after microsphere embolism in rats. Stroke 24, 415–420.

Takagi, N., Miyake, K., Ohiwa, A., Nukaga, R., Takeo, S., 1996. Effects of delayed treatment with nafronyl oxalate on microsphere-induced changes in monoamine levels of rat brain regions. Br. J. Pharmacol. 118, 33–40.

Takagi, N., Miyake, K., Taguchi, T., Tamada, H., Takagi, K., Sugita, N., Takeo, S., 1997. Failure in learning task and loss of cortical cholinergic fibers in microsphere-embolized rat. Exp. Brain Res. 114, 279–287.

Takeo, S., 1991. Time course of changes in acetylcholine and amino acids in the regional brain after microsphere-induced cerebral ischemia. Jpn. J. Pharmacol. 55 (Suppl. I), 67.

Takeo, S., Miyake, K., Minematsu, R., Tanonaka, K., Konishi, M., 1989. In vitro effect of naftidrofuryl oxalate on cerebral mitochondria impaired by microsphere-induced embolism in rats. J. Pharmacol. Exp. Ther. 2248, 1207–1214.

Takeo, S., Tanonaka, R., Miyake, K., Tanonaka, K., Taguchi, T., Kawakami, K., Ono, M., Hiramatsu, M., Okano, K., Minematsu, R., Konishi, M., 1991. Naftidrofuryl oxalate improves impaired brain glucose metabolism after microsphere-induced cerebral embolism in rats. J. Pharmacol. Exp. Ther. 257, 404–410.

Takeo, S., Taguchi, T., Tanonaka, K., Miyake, K., Horiguchi, T., Takagi, N., Fujimori, K., 1992. Sustained damage to energy metabolism of brain regions after microsphere embolism in rats. Stroke 23, 62–68.

Yamakuni, T., Usui, H., Iwanaga, T., Kondo, H., Odani, S., Takahashi, Y., 1984. Isolation and immunohistochemical localization of a cerebellar protein. Neurosci. Lett. 45, 235–240.

Zivin, J.A., Fisher, M., DeGirolami, U., Hemenway, C.C., Stashak, K.A., 1985. Tissue plasminogen activator reduces neurological damage after cerebral embolism. Science 230, 1289–1292.